International Space Planes and Hypersonic Systems and Technologies Conferences
6-9 March 2017, Xiamen, China
21st AIAA International Space Planes and Hypersonics Technologies Conference

10.2514/6.2017-2199

Effects of Shock Impingement on Aerothermal and Aerodynamic Performance for High-pressure Capturing Wings

Guang-li Li[1], Kai Cui[2], Yao Xiao[3] and Ying-zhou Xu[4]
LHD of Institute of Mechanics, Chinese Academy of Sciences, Beijing, China, 100190
School of Engineering Science, University of Chinese Academy of Sciences, Beijing, China, 100049

The high-pressure capturing wing (HCW) is a novel device that can improve the aerodynamic performance for large volume high-speed aircrafts. In hypersonic flows, the sharp leading edge of HCW must be blunted because of the severe aerothermal load. The oblique shock induced by body intersects to the bow shock induced by HCW. This paper proposes three cases based on the shock interaction location and studies the corresponding aerodynamic and aerothermal performance by numerical simulation under Mach 6 and zero angle of attack. The results show that the maximal heat flux and drag coefficient of HCW is determined by the interaction location. When the shock impinges on the inside of HCW, the shock boundary layer interaction occurs which lead to the increase of local heat flux on the lower surface of HCW. However, the maximal heat flux is almost the same with the freestream stagnation-point heat flux. The local extreme heat flux in the lower surface of HCW is about 20 percentage of the freestream stagnation-point heat flux. The drag coefficient is almost the same with freestream drag coefficient. When the shock impinges on the HCW leading edge, the type IV interference appears which could cause high pressure and heat flux on the surface. The non-dimensional maximal heat flux is about 3.5 and the maximal drag coefficient is about 1.8 in this case. When the oblique shock impinges on the outside of HCW, the non-dimensional maximal heat flux is about 1.5 and the drag coefficient is about 2.7.

Nomenclature

Ma	=	Mach number
R	=	Radius of HCW blunted leading edge, mm
y	=	Location of the impinging oblique shock wave, mm
P	=	Pressure, Pa
Q	=	Heat flux, MW/m^2
Cd	=	Drag coefficient
IS	=	Impinging oblique shock
BS	=	Bow shock
T	=	Temperature, K
SBLI	=	shock boundary layer interaction

Subscripts

st	=	Stagnation point
w	=	wall

[1] Gradute Student, LHD of Institute of Mechanics, Chinese Academy of Sciences, Beijing, 100190, China
[2] Associate Professor, LHD of Institute of Mechanics, Chinese Academy of Sciences, Beijing, 100190, China, kcui@imech.ac.cn
[3] Gradute Student, LHD of Institute of Mechanics, Chinese Academy of Sciences, Beijing, 100190, China
[4] Gradute Student, LHD of Institute of Mechanics, Chinese Academy of Sciences, Beijing, 100190, China

I. Introduction

The aerodynamic heating problem must be considered in the design of hypersonic aircraft configurations. Under hypersonic flight conditions (generally Mach number larger than 5), the leading edge suffers from serious aerothermal problems [1, 2]. The direct blunting technique, which is also the simplest and effective technique, is most commonly used to obtain acceptable heating levels [3]. As for the blunted leading edge of forebody, the peak heat flux is located in the stagnation point. Theoretical self-similar solutions [4, 5], experimental results [6] and some semi-empirical analyses [7] have all supported that the heat flux of stagnation point is inversely proportional to the root of the radius.

Regarding the blunted wing leading edge or inlet cowl-lip which is influenced by the forebody shock, the aerothermal problems are more complex. The shock interference and shock boundary layer interaction appear when the forebody oblique shock intersects the bow shock. These phenomena have been widely studied since the 1960s. Edney [8] formulated a detailed study of shock interference patterns and defined six types (Type I-IV) which are determined by the intersecting location of the impinging oblique shock relative to the bow shock. Subsequently, some research [9, 10] suggests that Type IV interference produces the most serious pressure and heat flux. This type causes a supersonic jet which leads to an extremely high pressure and heat flux. Until now, the problem is still attracted lots of concern by researchers.

To improve the aerodynamic performance as well as to relieve the contradiction between L/D and the volume for a high-speed flight vehicle, a novel device named high-pressure capturing wing was proposed in [11]. The HCW is mounted upon the body as a means of increasing lift through the two compressions of the body and HCW. The thickness of HCW could be very small relative to the body, so the additional drag is also small in zero angle of attack. Therefore the lift-to-drag ratio can be greatly increased due to the attachment of HCW. Similar to the hypersonic inlets, the HCW also needs pre-compression by forebody. The complex flow phenomena induced by shock interference and shock boundary layer interaction occurs near the HCW leading edge. The intersecting location of the impinging oblique shock can result in a big difference for the aerothermal performance, as well as the aerodynamic performance of HCW. Based on numerical simulation, this paper discusses the effect of different intersecting location of the impinging oblique shock on the aerothermal and aerodynamic performance of the HCW and provides a database for the HCW design.

II. Description of the Model

The effects of shock impingement on aerothermal and aerodynamic performance are explored by taking a family of wedges as vehicle bodies on the basis of two dimensional simulations. The oblique shock impinges on the bow shock can be classified into three categories, as shown in Figure 1. IS, BS denotes impinging shock, bow shock (undisturbed), respectively. In case 1, the shock impinges on the inside of HCW (sketched in Figure 1a). The HCW leading edge is almost in the freestream condition. Besides, the shock wave boundary layer interaction will occur in the lower surface of HCW. And in case 2, the shock impinges on the HCW leading edge (sketched in Figure 1b). The strong shock wave interactions will appear near the HCW leading edge. While in case 3, the shock impinges on the outside of HCW (sketched in Figure 1c). The whole HCW device is behind the oblique shock.

Each model consists two parts (sketched in Figure 1): the body and HCW. The wedge angle is defined as 9° . The radius of HCW leading edge is 1mm. The distance between the HCW and body is varied to choose different cases of impingement shock. A freestream Mach number of 6, flight height of 26km, and angle of attack of 0° have been used

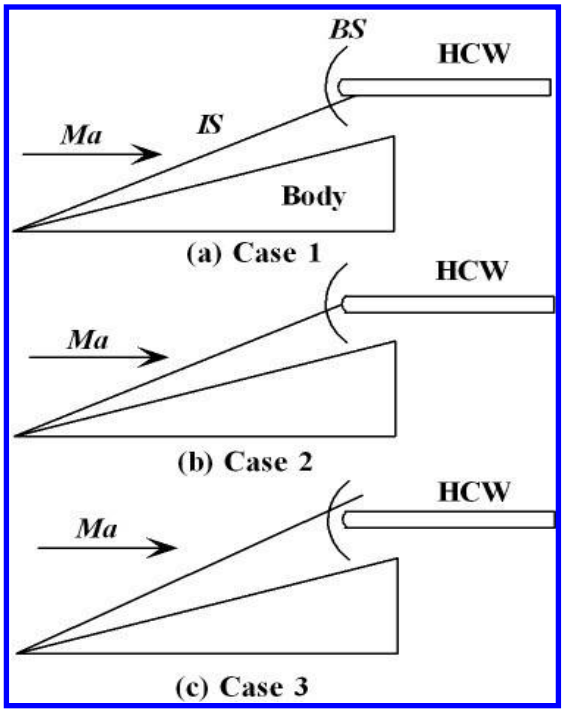

Figure 1. Description of the model

as flow conditions. The temperature of wall is isothermal-constant: T_w=294.44K. Numerical solutions are calculated by solving the compressible Navier-Stokes equations with the use of a second order total variation diminishing (TVD) scheme for spatial discretization. A second order implicit time marching scheme and laminar model are used in the computations.

The position of impinging shock wave induced by wedges body is expressed by y, as shown in Figure 2, and the leading edge point location of the HCW is expressed by θ. The different y value is corresponding to the different intersecting location of the impinging shock relative to the bow shock which directly determines the aerothermal and aerodynamic performance for the HCW. The value of y/R corresponding to case1, case 2, and case3 is less than -1, greater than -1 and less 1, and greater than 1, respectively. In this paper, different y/R values are simulated for the analysis of three cases above.

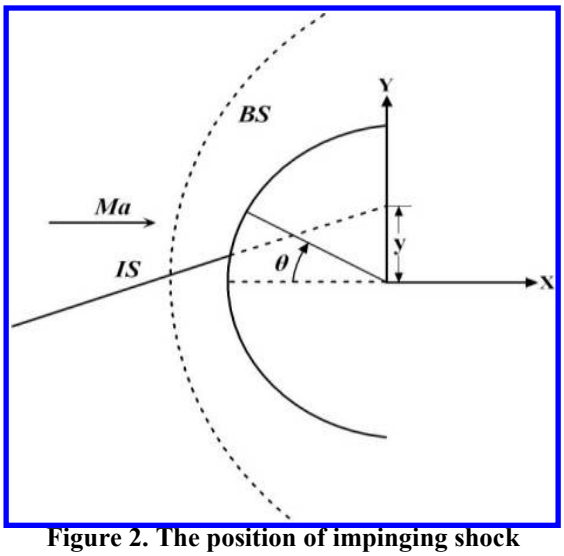

Figure 2. The position of impinging shock

III. Results and Discussions

A. Flow characteristics of the different shock interaction locations

The different interaction location is defined by the oblique shock impingement on the center vertical direction, as described in Figure 2. The non-dimensional parameter is y/R. The conditions of y/R=-2, -1, 0, 0.25, 0.5, 2 are carried out for the current study. Figure 3 illustrates the Mach number contours for all cases. It can be found that Figure 3a y/R=-2 is corresponding to case 1. The shock impinges on the inside of HCW. Figure 3b-d y/R=-1, 0, 0.25, 0.5 are corresponding to case 2 in which the shock impinges on the leading edge. Figure 3f is corresponding to case 3 in which the shock impinges on the outside of HCW.

For y/R=-2, the oblique shock intersects below the lower sonic line of the undisturbed bow shock. Two reflection shock waves and shear layer are formed as shown in Figure 3a. The shear layer is between the two reflection shock waves. The upper reflection shock impinges on the lower surface of HCW which generate the shock boundary layer interaction (SBLI) problems. Two shock waves are formed in the separation and reattachment points of the separation bubble. The leading edge of HCW is influenced by the freestream. So the impinging shock wave mainly has effect on the lower surface of the HCW, but little effect on the edge surface.

For y/R=-1, the interaction location is close to the lower sonic line. The strength of the oblique shock is much weaker than that of the bow shock. Under this condition, a reflection shock and a shear layer is formed, as shown in Figure 3b. The shear layer does not impinge on the leading edge and flows into the downstream. As the oblique shock wave move upward, when y/R=0, different from y/R=-1, the shear layer encounters the surface of leading edge. From Figure 3d, the oblique shock intersects the subsonic region of the bow shock. A supersonic jet is produced in the subsonic flow. The jet impinges on the leading edge surface and ends up with a normal shock. This condition is known as the Type IV shock interference pattern which is defined by Edney [8]. When y/R=0.5, the supersonic jet region moves upward. The flow characteristic is similar to the condition of y/R=0.25.

From y/R=2, as shown in Figure 3f, the oblique shock intersects above the sonic line of the bow shock which produces the Type V shock interference pattern defined by Edney. A triple shock type and a shear layer are formed above the HCW upper surface. The shear layer does not impinge on the upper surface of the HCW. The whole leading edge of HCW is behind the oblique shock wave. The bow shock of the leading edge is compressed by the flow field behind the oblique shock.

The different shock interaction locations induce significant alterations in the flow characteristic around the leading edge and the surface of the HCW, including the shock/shock interactions and the shock boundary interactions. These different patterns will affect the pressure and the heat flux of the HCW.

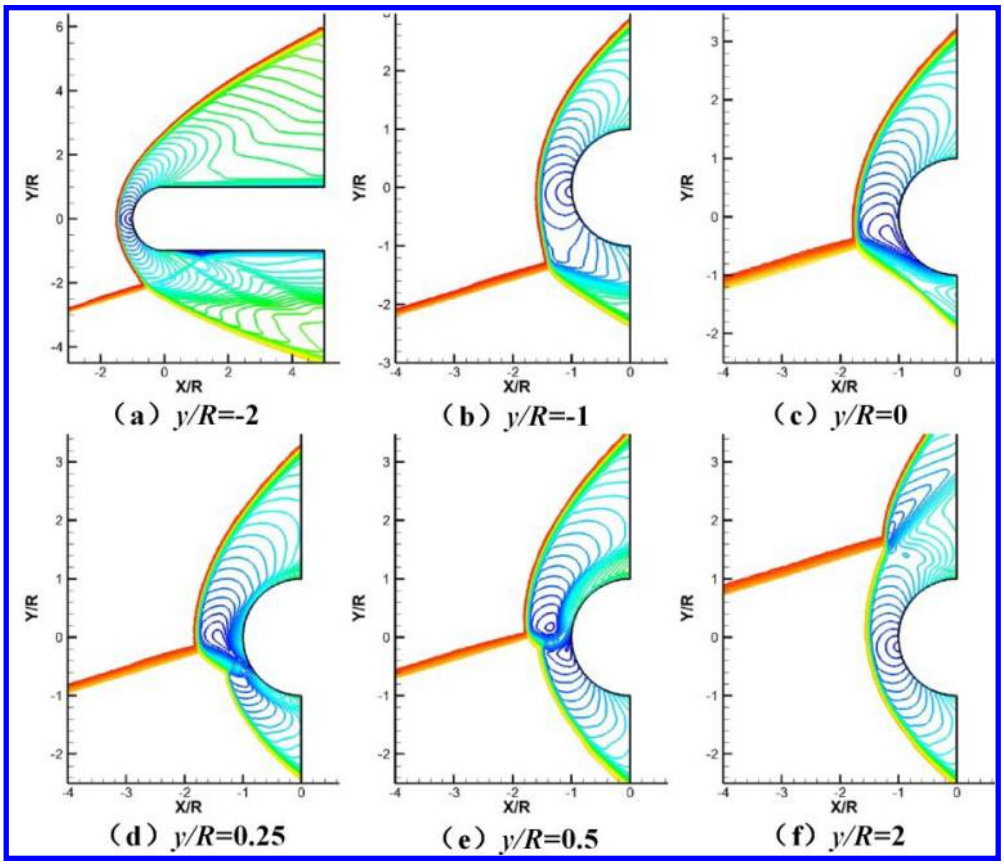

Figure 3. Mach contours near the HCW leading edge with different impingement shock

B. The pressure and heat flux on the leading edge of HCW

The corresponding pressure and heat flux on the leading edge of HCW are illustrated in Figure 4 and Figure 5, respectively. In figure 4, the pressure P on the surface is non-dimensioned with respect to the stagnation-point pressure without shock interaction in the same conditions. In Figure 5, the heat flux Q on the surface is non-dimensional with respect to the stagnation-point heat flux without shock interaction in the same condition. The different position point of the leading edge surface is expressed by θ as mentioned in Figure 2.

Under the condition of y/R=-2, the airflow of the HCW leading edge is freestream. So the pressure and heat flux distribution is similar to the condition of without shock interaction. There exist local pressure and heat flux extreme value point near the SBLI, as shown in Figure 6. However, they are both small with respect to the stagnation-point. The local extreme pressure and heat flux in the lower surface of HCW are both about 20 percentage of the freestream stagnation-point heat.

For y/R=-1, the bow shock is influenced by the shock interaction. The pressure and heat flux on the lower surface of leading edge have a small increase, and the pressure and heat flux on the upper surface of leading edge have a small decrease, relative to the condition of y/R=-2. Under the condition of y/R=0, the shear layer impinges on the leading edge. The pressure and heat flux increase obviously near the impinged region. While under the condition of y/R=0.25 and y/R=0.5, the pressure and heat flux increase dramatically because of the supersonic jet.

As the intersection location moves upward, the value y/R=2, the whole leading edge is behind the oblique shock. Therefore, the pressure and heat flux have a certain increase in all points. The bow shock shape before the edge is relatively similar to the undisturbed bow shock, but more close to the surface. The shear layer has a weak effect on the upper surface of the leading edge.

As discussed above, the shock interaction location has a significant effect on the pressure and the heat flux distributions. The peak heat flux is all formed in the leading edge for all cases. It also determines the drag of the leading edge of HCW.

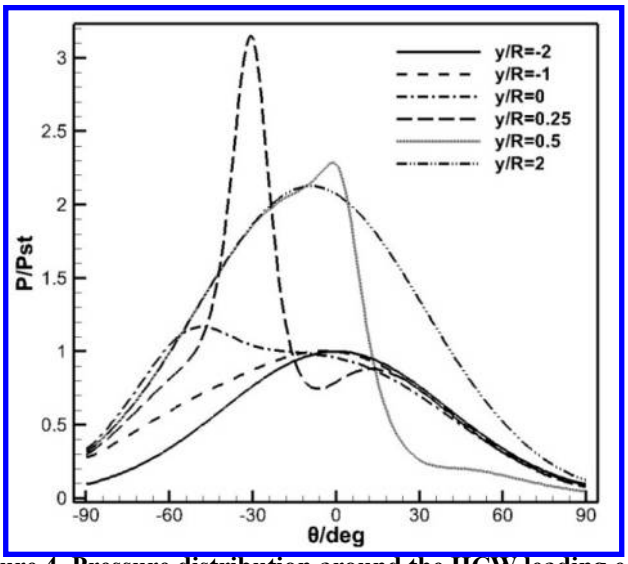

Figure 4. Pressure distribution around the HCW leading edge

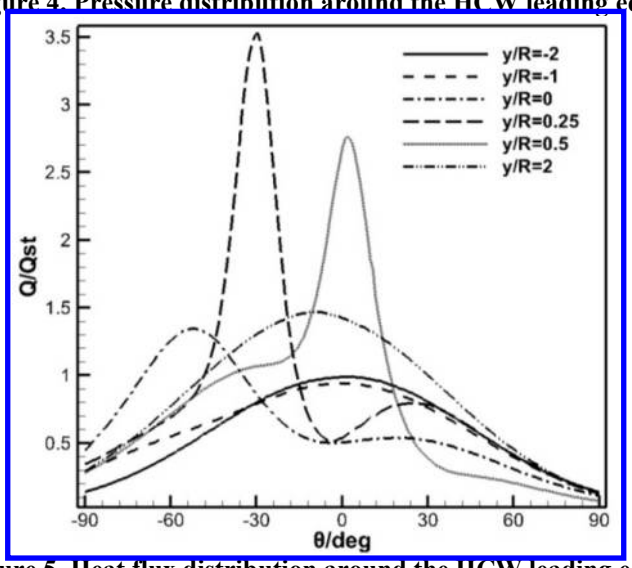

Figure 5. Heat flux distribution around the HCW leading edge

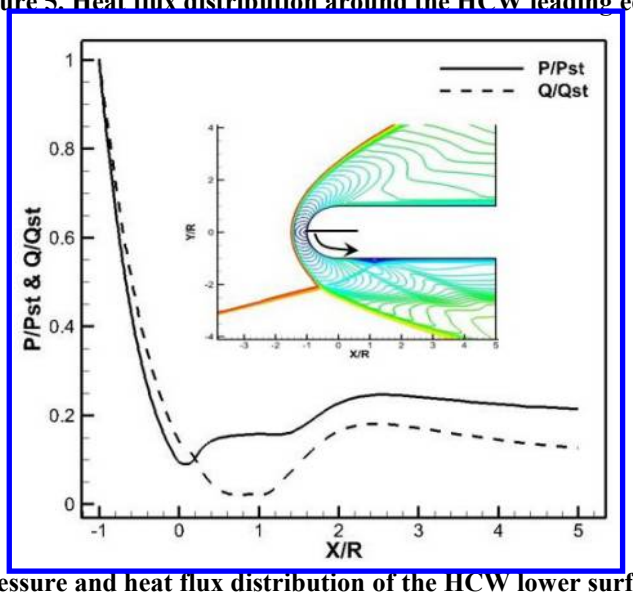

Figure 6.Pressure and heat flux distribution of the HCW lower surface, y/R=-2.

C. The maximal heat flux and drag coefficient

From the flow characteristics of the different shock interaction locations discussed above, we can find that the maximal heat flux occurs on the leading surface of HCW for all cases. The whole drag of the HCW includes two parts. One is the drag of leading edge, the other one is the drag of upper surface and lower surface. However, in the design condition of zero angle of attack, the upper surface and lower surface only produce viscous drag, and the wave drag is produced only by the leading edge which is much bigger than the viscous drag. Therefore, the wave drag of the leading edge of HCW is discussed here for simplification. The drag coefficient here is non-dimensioned by radius of HCW leading edge.

The maximal heat flux and drag coefficient against the value of y/R are plotted in Figure 7. From the *Cd* line, we can find that the *Cd* value increases along with the interaction location moves upward. The minimal *Cd* occurs in y/R=-2, and the value is 1.27. The maximal *Cd* occurs in y/R=2 and the value is 2.71, which is about 2 times bigger than the minimal value. So the drag of the HCW is very sensitive to the shock interaction locations. Additionally, the maximal heat flux corresponding to the y/R=-2, -1, 0, 0.25, 0.5 and 2 is respectively 1, 0.94, 1.35, 3.53, 2.76 and 1.47 times of the stagnation point heat flux, as illustrated in Figure 7. The difference of the maximal heat flux is attributed to the different flow characteristics induced shock interaction as described in above section. The minimal one of these maximal heat flux is 0.94 under the condition of y/R=-1, and the maximal one is 3.53 under the condition of y/R=0.25. So the maximal heat flux of the HCW is also sensitive to the shock interaction locations.

According to the classified methods in Figure 1, the shock impinges on the inside of HCW in case 1. The shock boundary layer interaction occurs on the lower surface of HCW which lead to the increase of the local heat flux. However, the maximal heat flux is almost the same with the freestream stagnation-point heat flux. The local extreme heat flux in the lower surface of HCW is about 20 percentage of the freestream stagnation-point heat flux. The drag coefficient is almost the same with freestream drag coefficient. In case 2, when the shock impinges on the HCW leading edge, the type IV interference appears which causes high pressure and heat flux on the surface. The non-dimensional maximal heat is about 3.53 times than the stagnation-point heat flux without shock interaction. The drag of HCW also has some increase. In case 3, when the oblique shock impinges on the outside of HCW, the non-dimensional maximal heat flux is about 1.5 and the drag coefficient is about 2.7. The drag is largest in the three cases for case 3, and the maximal heat flux is largest in case 2. In case 1, the maximal heat flux and drag are both least.

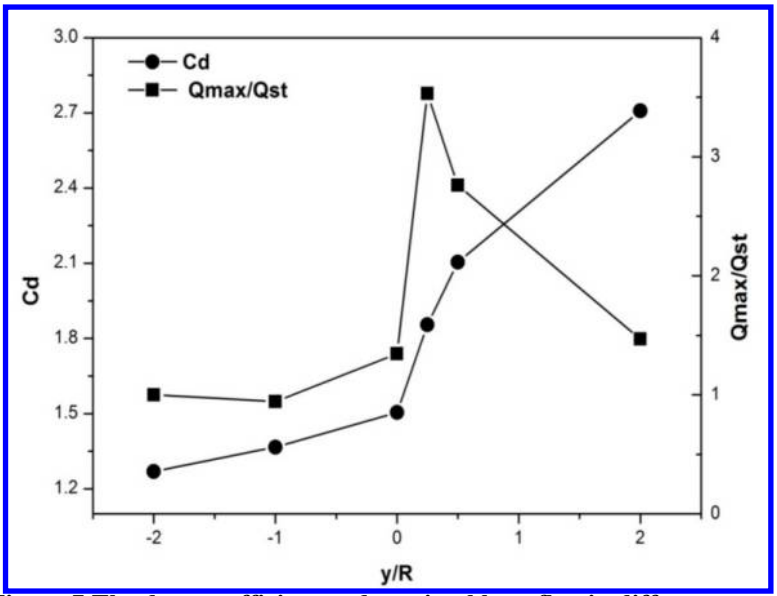

Figure 7.The drag coefficient and maximal heat flux in different types.

IV. Conclusion

Three cases of shock interactions for high-pressure capturing wings are calculated in this paper. The flow characteristics of the different shock interaction locations are studied. The pressure and heat flux distributions on the leading edge of HCW is analyzed. Furthermore, the drag coefficient and maximal heat flux corresponding to three cases are discussed.

Among the three cases, we find that the case 1 is best for both the aerothermal and aerodynamic performance. The drag and maximal heat flux is almost the same as the freestream conditions. In this case, shock interaction has

little effect on the leading edge of HCW. In case 2, there exists Type IV shock interference pattern which may lead significant increase of drag and heat flux, so we should avoid this case in the design of high-pressure capturing wing configurations. In the last case, the whole HCW is behind the oblique shock. So the drag and heat flux have some increase than case 1. Overall, case 1 is the best for the aerothermal and aerodynamic performance. However, there exists the shock boundary layer interaction problem in the lower surface of HCW. It leads to the increase of the pressure and heat flux near the separation regions. This must be considered for actual design.

Acknowledgement

This research was funded by the National Natural Science Foundation of China (NSFC) under grant numbers 11372324 and 11572333.

References

[1]Bertin, J, J., "Hypersonic Aerothermodynamics," Washington, DC: AIAA, 1994. 240-267
[2]Anderson, J, D., "Hypersonic and High Pressure Gas Dynamics," 2nd ed. Reston, VA: AIAA, 2000. 346-355
[3] Cui, K., Hu, S, C., "Shape Design to Minimize the Peak Heat-Flux of Blunt Leading-edge," AIAA Paper, AIAA-2013-0233
[4]Driest, E.R.V., "The problem of aerodynamic heating," Aeronautical Engineering Review, Vol.15, No.10, 1956, pp, 26-41
[5]Fay, J.A., Riddell, F.R., "Theory of stagnation point heat transfer in dissociated air," Journal of the Aeronautical Sciences, Vol. 25, 1958, pp. 73-85
[6] Rose, P.H., Stankevices, J.O., "Stagnation point heat transfer measurements in partially ionized air," AIAA Journal, Vol. 1, No. 12, 1963, pp. 2752-2763
[7]Sutton, K., Graves, R.A., "A general stagnation-point convective-heating equation for arbitrary gas mixtures," National Aeronautics and Space Administration, 1971
[8]Edney, B., "Anomalous Heat Transfer and Pressure Distributions on Blunt Bodies at Hypersonic Speeds in the Presence of an Impinging Shock," Technical Report, FFA 115, Aeronautical Research Institute of Sweden, 1968
[9]Wieting, A.R., Holden, M.S., "Experimental study of shock wave interference heating on a cylindrical leading edge at Mach 6 and 8," AIAA Journal, 1989, 27(11): 1557-1565
[10]Brorovoy, V., Chinilov, A., Gusev, V., et al. "Interference between a cylindrical bow shock and a plane oblique shock," AIAA Journal, 1997, 35(11): 1721-1728
[11]Cui, K., Li, G.L., Xiao, Y., "Aerodynamic Performance Study of High Pressure Capturing Wing Configurations," AIAA Paper, AIAA-2015-3388